Optimum Traction Force Distribution for Stability Improvement of 4WD EV In Critical Driving Condition

Peng He
The University of Tokyo
Department of Electrical Engineering
4-6-1 Komaba, Meguro, Tokyo 153-8505, Japan
ka@horilab.iis.u-tokyo.ac.jp

Yoichi Hori
The University of Tokyo
Institute of Industrial Science
4-6-1 Komaba, Meguro, Tokyo 153-8505, Japan
hori@iis.u-tokyo.ac.jp

***Abstract*— This paper is concerned with integrated yaw stability control strategy for 4WD EV driven by in-wheel motors. The strategy consists of double control loops. One is the upper control loop, which uses $2-DOF$ control method to specify control effectors which are required for keeping EV yaw stability. The other is the lower control loop, which is used to determine control inputs for four driving motors by optimum traction force distribution method. This distribution method is implemented by redundancy control.**

The simulation results indicate that handling stability of this 4WD EV is improved by proposed strategy, especially when the EV drives in critical conditions.

I. Introduction

In order to improve maneuverability, stability and obtain much more driving traction force, many electric vehicles (EVs) are equipped with more than two actuating motors.

Further, the power transfer construction of EV is changed days after days. The latest EV is driven by four motorized wheels, which mean driving motors are fitted into wheels and can be controlled independently[1][2].

For example, ”UOT March II”, which is shown in Fig.1, has four in-wheel driving motors (4WD). Control strategies, such as ABS, TCS and VSC, can be implemented for that EV easily by advanced motion control of in-wheel electric motors.

Fig. 1. ”UOT March II” and in-wheel motors.

For planar motion control of EV, yaw rate and side slip angle are often chosen to be controlled. However, the control methods, such as in the paper[3], have contributed in improving vehicle performance and guaranting safety for 2WD vehicles, which means that vehicle has two driving wheels.

However, in 4WD case, due to four driving motors, control system has four permitted independent control inputs[4]. And those control inputs are all avaiable to control yaw rate and side slip angle. Because the number of indepent control inputs much than the number of controlled variables, therefore, there is an actuator redundancy problem[5].

If we design control laws for 4WD EV, one issue which must be faced is how to deal with such actuator redundancy, which means how to distribute traction force for four driving motors.

Further, in order to avoid slip or lock and keep stability, especially when EV drives in critical conditions, distributing traction force should consider the conditions of tire friction.

When 4WD EV drives in critical or dangerous conditions, even if one driving motor failures, the redundancy of control inputs can be used to deal with those things and avoid instability.

In this paper, we discuss a method optimally and dynamically to distribute traction force by actuator redundancy control, which permits us to consider constraints of actuating motors (limitation of tire friction force). The ”optimally” means the best combination of redundant set of actuators. The ”dynamically” means the resolution depends not only on the current conditions but also on the previous sampling instant.

By using that optimum traction force distribution, we also propose an integrated yaw stability control algorithm for 4WD EV. As Fig.3 shows, the strategy consists of double control loops. The upper control loop composes optimal feedback control and yaw moment feedforward control. The lower control loop is dynamic traction force distribution control. This loop is used to calculating control inputs for four driving motors. In this loop, an actuator redundancy problem is resolved.

The remainder of this paper is organized as follows: in section 2, 4WD EV modeling is mentioned; in section 3, integrated yaw stability control algorithm for 4WD EV is

discussed; in section 4, application of proposed algorithm for improving stability of 4WD EV in critical driving is discussed; in last section, preliminary conclusions and future works are mentioned.

II. 4WD EV Modeling

In order to design control law for 4WD EV ("UOT March II"), a linear model is used, which is abstracted from the EV shown in Fig.1. The model is described in Fig.2. We assume that only front wheels can be steered and steering angles of front wheels are equal to each other. In Fig.2, δ_f is the steering angle. V is the velocity vector of center of gravity (COG) of EV. All F_{ij} mean traction forces. β represents sideslip angle of COG. γ represents yaw rate of COG. M_z is yaw moment. β and γ are controlled output variables. M_z and δ_f are control inputs. The state equation is given by Eq.1[6][7].

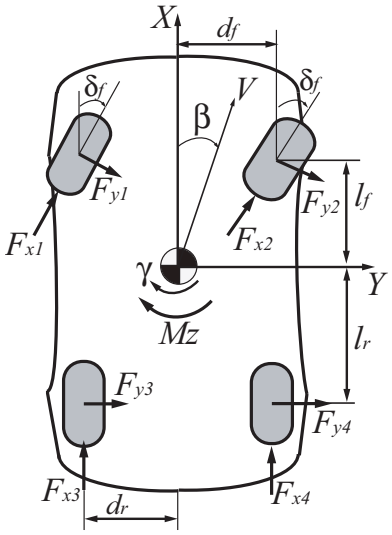

Fig. 2. Linear vehicle model for dynamic analysis

$$\begin{pmatrix}\dot{\beta}\\ \dot{\gamma}\end{pmatrix} = \underbrace{\begin{bmatrix}a_{11} & a_{12}\\ a_{21} & a_{22}\end{bmatrix}}_{A}\begin{pmatrix}\beta\\ \gamma\end{pmatrix} + \underbrace{\begin{bmatrix}b_{11} & b_{12}\\ b_{21} & b_{22}\end{bmatrix}}_{B}\begin{pmatrix}\delta_f\\ M_z\end{pmatrix} \quad (1)$$

where

$$A = \begin{bmatrix} -\frac{2(C_f+C_r)}{MV} & -1-\frac{2(l_fC_f-l_rC_r)}{MV^2} \\ -\frac{2(l_fC_f-l_rC_r)}{I_z} & -\frac{2(l_f^2C_f+l_r^2C_r)}{I_zV}\end{bmatrix}$$

$$B = \begin{bmatrix} \frac{2C_f}{MV} & 0 \\ \frac{2l_fC_f}{I_z} & \frac{1}{I_z}\end{bmatrix}$$

M is the vehicle mass. I_z is the inertia moment. C_f (C_r) is the cornering stiffness of front (rear) tire. l_f (l_r) is the distrance from the front (rear) axial to the COG.

The transfer functions from steering angle δ_f and yaw moment M_z to yaw rate γ are

$$\begin{aligned}\gamma &= \frac{G_\gamma(0)(1+T_\gamma s)}{1+\frac{2\zeta}{\omega_n}s+\frac{1}{\omega_n^2}s^2}\delta_f + \frac{G_M(0)(1+T_M s)}{1+\frac{2\zeta}{\omega_n}s+\frac{1}{\omega_n^2}s^2}M_z \quad (2)\\ &= G(s)\delta_f + H(s)M_z\end{aligned}$$

where, $G_\gamma(0)$ and $G_M(0)$ are steady gains. $G_\gamma(0) = \frac{V}{l}\frac{1}{1+KV^2}$ and $G_M(0) = \frac{V(C_f+C_r)}{2l^2C_fC_r(1+KV^2)}$. T_γ and T_M are time constants. $T_\gamma = \frac{Ml_fV}{2lC_r}$ and $T_M = \frac{MV}{2(C_f+C_r)}$. l is the length of chassis ($l = l_f + l_r$). K is the stability factor of EV, $K = -\frac{M}{2l^2}\frac{l_fC_f-l_rC_r}{C_fC_r}$.

ζ is the damping coefficient. ω_n is the natural frequency of control system.

$$\omega_n = \frac{2l}{V}\sqrt{\frac{C_fC_r}{MI_z}}\sqrt{1+KV^2} \quad (3)$$

$$\zeta = \frac{M(l_f^2C_f+l_r^2C_r)+I_z(C_f+C_r)}{2l\sqrt{MI_zC_fC_r(1+KV^2)}} \quad (4)$$

III. Integrated Yaw Stability Control Algorithm

The concept of the proposed control algorithm is shown in Fig.3. The reference input commands are $X_1, ..., X_p$. The control inputs for motors are $U_1, ..., U_n$ and the controlled output variables of EV are $Y_1, ..., Y_p$. The upper control loop composes optimal states feedback control and yaw moment feedforward control. This control loop is used for calculating "virtual" control effectors $V_1, ..., V_m$, which is required for realizing steady and dynamic characteristics of control system. However, the "virtual" control effectors could not directly be control inputs $(U_1, ..., U_n)$ for motors. Therefore, in the lower control loop, we map the "virtual" control effectors to physical control inputs for motors by optimum dynamic traction force distribution. Then we control EV to achieve the "virtual" control effectors by traction force control of in-wheel motors. The traction force distribution is implemented by redundancy control.

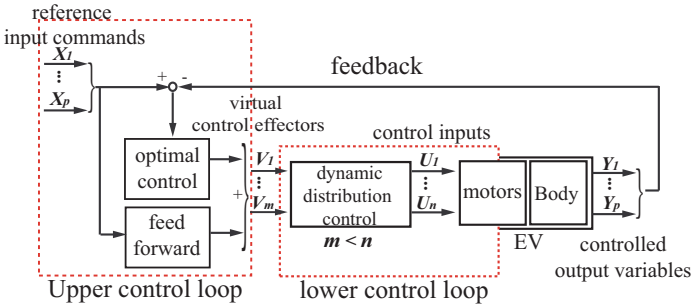

Fig. 3. Block diagram of control strategy for EV

For planar motion control of 4WD EV, steering angle δ_f and accerelation pedal angle θ are given by driver. And then, a reference model is used for calculating reference input commands γ^* and β^* in accordance with driver's commands. The controlled output variables are yaw rate γ and slip angle β. The "virtual" control effectors are yaw moment M_z and active steering angles. The physical control inputs are traction force commands for motors.

In this study, θ is assumed to be zero and reference input command is only γ^*. The "virtual" control effector is yaw moment M_z.

The upper control loop includes reference model control, feedforward control which is designed as a $P-$ controller, feedback control which is designed by using a **LQG** regulator. Therefore, robust "2-DOF" control algorithm is used for the design of upper control loop.

The lower control loop consists of dynamic optimal traction force distribution, which is used to determine control inputs for motors according to "virtual" control effector and tire friction conditions.

The control objective is to make the EV to follow the desired yaw rate.

A. Reference model

According to Eq.2, yaw rate response from steering angle of "UOT March II" is shown in Fig.4.

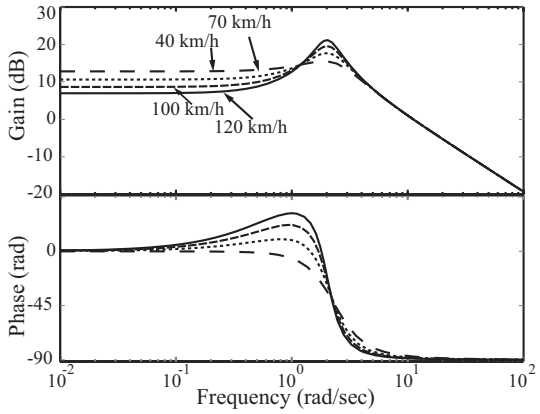

Fig. 4. Yaw response of "UOT March II"

In order to improve yaw rate phase delay and thus make lateral response quick, the reference model is defined as follow

$$\gamma^* = G(s)_{ref}\delta_f = \frac{G_\gamma(0)(1+T_\gamma s)}{1+\frac{2\zeta}{\omega_n'}s+\frac{1}{\omega_n'^2}s^2}\delta_f \tag{5}$$

where γ^* is the target yaw rate. We make reference model to have quick response, which means $\omega_n' > \omega_n$. In this study, we put $\omega_n' = 1.5\omega_n$. The response is shown in Fig.5.

B. Feedforward control

According to Eqs.2 and 5, in order to make the real yaw rate of EV fit the target value, we calculate the required yaw moment M_{ff} as one part of "virtual" control effector M_z[6].

$$\gamma^* - \gamma = G(s)_{ref}\delta_f - G(s)\delta_f - H(s)M_{ff} = 0 \tag{6}$$

$$M_{ff} = \frac{G(s)_{ref} - G(s)}{H(s)}\delta_f \tag{7}$$

Based on Eq.7, feedforward control law is designed as a $P-$ controller

$$P = \frac{G_\gamma(0)T_\gamma}{G_M(0)T_M}\frac{\omega_n'^2 - \omega_n^2}{\omega_n^2} = 2l_fC_f(\frac{\omega_n'^2}{\omega_n^2} - 1) \tag{8}$$

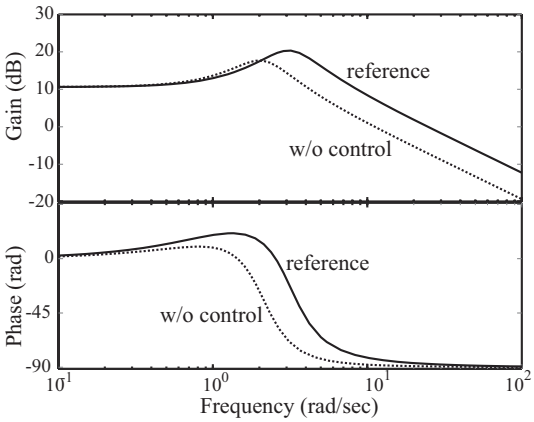

Fig. 5. Yaw response of reference model ($V = 60km/h$)

C. Feedback control

However, due to inaccuracy of EV model and effect of disturbance, Eq.8 is incomplete to satisfy Eq.7. For example, C_f, which is the cornering power of front tire, changes in real time. It is difficult for us to know its true value. Therefore, we compensate the "P-" controllor by using a **LQG** regulator. The controlled variables are γ and β. The **LQG** regulator is designed as follows

$$\min\ J = \int_0^\infty (\mathbf{E}^T Q\mathbf{E} + M_{fb}^T R M_{fb})dt \tag{9}$$

where Q and R are weighting matrices and decided according to experiments. $\mathbf{E} = (\gamma^* - \gamma, \beta^* - \beta)^T$. Yaw moment M_{fb} is another part of "virtual" control effector M_z.

We can calculate M_{fb} by

$$M_{bf} = -K\mathbf{E} \tag{10}$$

$$K = R^{-1}B^TS \tag{11}$$

where S is the solution of Algebraic Ricatti Equation

$$A^TS + SA + Q - SBR^{-1}B^TS = 0 \tag{12}$$

D. Optimum traction force distribution

In 4WD case, four driving motors can be used for motion control. As Fig.6 shows, the inputs of lower control loop are yaw moment M_z and driving force F_{ac} (F_{ac} is assumed to equal to total friction force). As mentioned above, the virtual control effector is yaw moment M_z, $M_z = M_{ff} + M_{fb}$.

According to virtual control effector M_z, dynamic optimal traction force distribution is used to determine control input commands for four motors to

- keep the tire from slipping or locking.
- obtain the maximum tire load ratio.
- achieve the control effectors.
- improve yaw rate stability.

According to Fig.2, if four tires are all in adhesion states, yaw moment M_r can be obtained by

$$M_r = d_fF_{x1} + d_rF_{x3} - d_fF_{x2} - d_rF_{x4} \tag{13}$$

where d_f and d_r are front and rear tread. $F_{x1}, F_{x2}, F_{x3}, F_{x4}$ are traction forces.

Optimum traction force distribution control is used to convert "virtual" control effector M_z to physical control inputs for available sets of motors. According to Eq.13, the distributed traction forces can realize yaw moment M_r in real time. By optimum traction force distribution control, the error between the "virtual" control effector M_z and the achieved real yaw moment M_r is to be minimized. Therefore, the required control objective will be obtained due to $M_r \approx M_z$. And at the same time, tire driving conditions are considered to keep tire from spinning or slipping.

Distribution control is generally used for solving this kind of problem. It is often used for flight control or marine vessel control[8][9]. It was also previously used for automotive control[10][11]. However, it was a static inverse mapping method[12]. Some resolutions mainly focus on how to easily implement or how to efficiently calculate for control system[12].

That means,

$$\min \|W_1 \mathbf{F}\|_2 \tag{14}$$

subject to $M_z = \mathbf{B_v} \cdot \mathbf{F}$.

Where W_1 is weighting matrix. $\mathbf{F} = (\tilde{F}_{x1}, \tilde{F}_{x2}, \tilde{F}_{x3}, \tilde{F}_{x4})^T$ are control input commands for motors. Virtual control vector $\mathbf{B_v} = (d_f, -d_f, d_r, -d_r)$.

Control inputs $\mathbf{F}$ are obtained by

$$\mathbf{F} = W_1^{-1}(\mathbf{B_v} W_1^{-1})^{\dagger} M_z \tag{15}$$

where † means pseudo-inverse of matrix.

In order to consider dynamics of tire friction, we try to extend the above static resolution to a dynamic optimum one. The "dynamic" means redundancy resolution which depends not only on the current conditions but also on the resolution of previous sampling instant[13].

According to Eq.13, Eq.14 is extended to

$$\min \|W_1 \mathbf{F}(t)\|_2 + \|W_2(\mathbf{F}(t) - \mathbf{F}(t-T))\|_2 \tag{16}$$

subject to $M_z = \mathbf{B_v} \cdot \mathbf{F}$. Where W_2 is weighting matrix too.

Control inputs $\mathbf{F}$ are obtained by

$$\mathbf{F}(t) = W_1^{-1}(\mathbf{B_v} W_1^{-1})^{\dagger} M_z + P\mathbf{F}(t-T) \tag{17}$$

where $P = (I - W^{-1}(\mathbf{B_v} W^{-1})^{\dagger} \mathbf{B_v}) \frac{W_2^2}{W^2}$, † means pseudo-inverse of matrix, $W^2 = W_1^2 + W_2^2$.

Eq.17 is just like a digital first order low pass filter, which means dynamic redundancy resolution $\mathbf{F}(t)$ can be obtained by filtering a desired or reference static value. It is this point that the change of frequency and extent of control inputs can be dynamically controlled quite well[13]. It is easy to verify that the eigenvalues of matrix P are bounded by 1, which means Eq.17 is asymptotically stable[13].

IV. Simulation

The actual control diagram is shown in Fig.6. In accordance with what mentioned above, the upper control loop uses "2-DOF" algorithm by integrating with yaw moment feedforward and states feedback control. The lower control loop is dynamic optimum traction force distribution control. The control objective is to make the EV to follow the desired yaw rate.

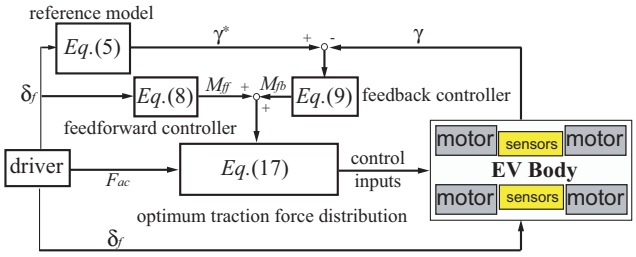

Fig. 6. Integrated yaw stability control algorithm for 4WD EV

The specifications of "UOT March II", which are used for simulations, are shown in TABLE I.

TABLE I
THE SPECIFICATIONS OF "UOT MARCH II"

Dimensions (L×W×H)		3695×1660×1525 (mm)
Weight		1100kg
Inertia moment		3.76×10^3 kgm^2
Tire Radius		0.26m
Motor (/unit)	Max. output	36kW
	Max. torque	77Nm
	Max. speed	8700rpm
	reduction gear	ratio 5.0
Battery	Type	Panasonic EC-EV1238
	Capacity	38Ah
	Voltage	12V × 19 modules

A. Verification

In order to verify the effectiveness and efficiency of the calculated virtual control effector, we performed two kinds of tests for EV (" UOT March II"). In this case, optimum traction force distribution control is not used.

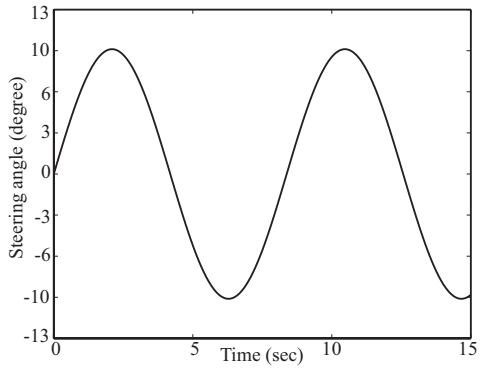

Fig. 7. Input signal for Lane change test of "UOT March II"

First, driver input singal and simulation result are shown in Figs.7 and 8, which show that the yaw rate can be controlled to well fit the reference value.

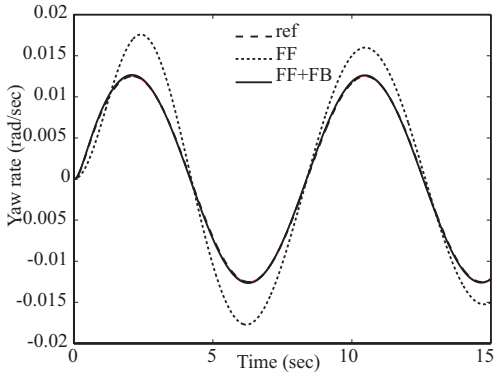

Fig. 8. Yaw response of "UOT March II" in lane change test ($V = 60km/h$)

The second test is "J turn" test. Driver input singal and simulation result are shown in Figs.9 and 10, which also show the effectiveness of control algorithm.

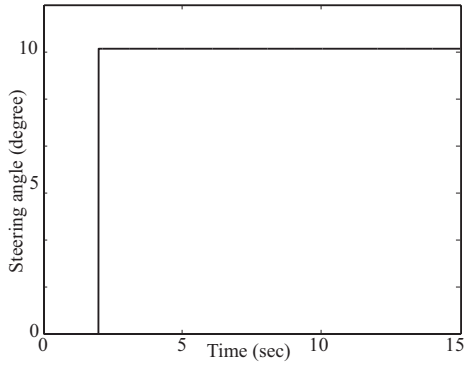

Fig. 9. Input signal for J-turn test of "UOT March II"

Therefore, it can be deduced that the upper control loop can give the quite right virtual control effector to satisfy the control requirement.

B. Comparison

Simulation is performed to compare the proposed control method with the one which does not use traction force distribution method. We use "Lane change" test for that comparison. In this case, the friction forces of left and right tire are different to each other. The friction coefficient of left side is 0.8, but right one is 0.3. It means that EV drives "Lane change" on a split μ road.

We suppose that the traction force distribution method which we want to compare is

$$M_r = d_r F_{x3} - d_r F_{x4} \tag{18}$$

As Fig.11 shows, control method which does not use optimum traction force distribution, can not make the controlled

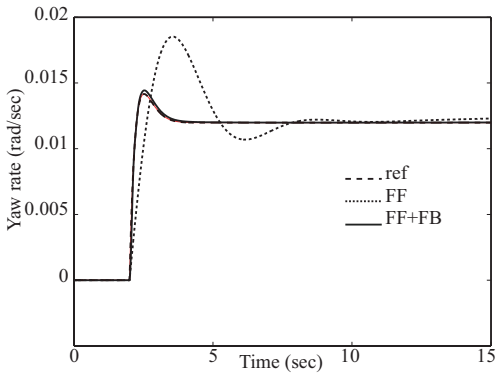

Fig. 10. Yaw response of "UOT March II" in J-turn test ($V = 60km/h$)

yaw rate to follow the reference value quickly and accurately. It cannot keep EV handling from instability.

On the contrary, as Fig.12 shows, when we use optimum traction force distribution control, which is realized by taking advantage of redundancy of control inputs, the controlled yaw rate can follow the reference value quite well. It means stability of EV can be improved.

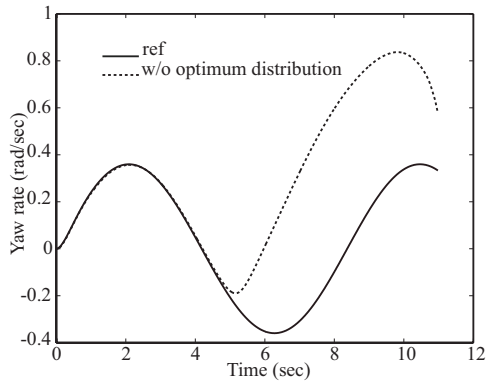

Fig. 11. Yaw rate response of EV on split μ road without optimum traction force distribution

As Fig.13 shows, when it does not take full advantage of the redundancy of control inputs for traction force distritution, the rear slip. It causes EV being instability, which is shown in Fig.15. For this case, the EV can not make "Lane change" under the test condition.

When redundancy of control inputs is considered and well used for optimum traction force distribution, the coorresponding tire slip ratio is kept in a safty domain, which is shown in Fig.14. For this case, the EV can realize stable "Lane change" under the same test condition.

V. Conclusions and Future Works

Simulation results show that the proposed control strategy can improve the stability of 4WD EV, especially EV drives in critical conditions. Optimum traction force distribution control can be an effective method when take full advantage of redun-

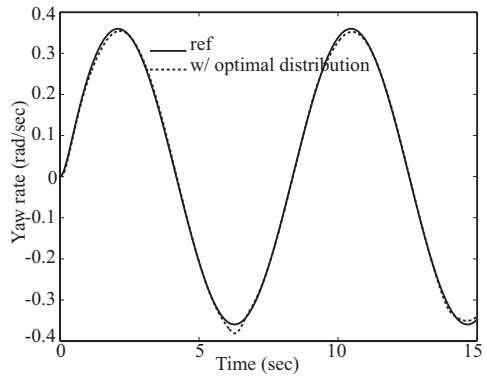

Fig. 12. Yaw rate response of EV on split μ road with optimum traction force distribution

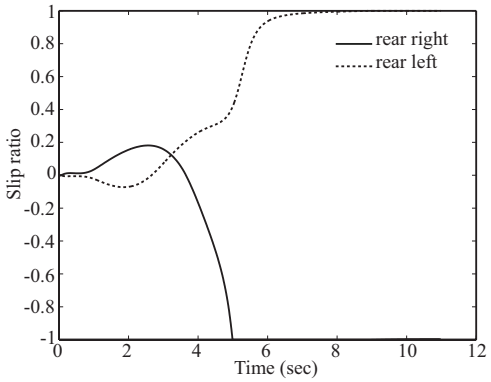

Fig. 13. Slip ratio of rear tires when optimum traction force control is not used

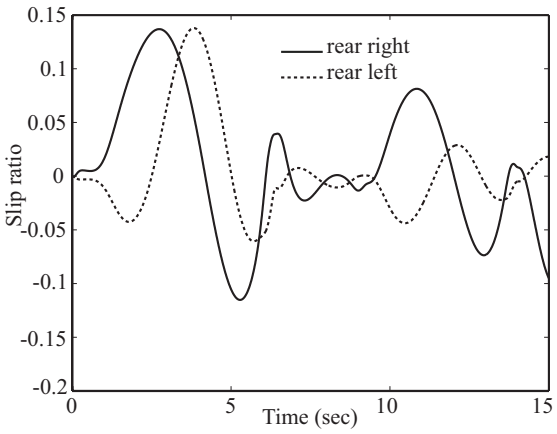

Fig. 14. Slip ratio of rear tires when optimum traction force control is used

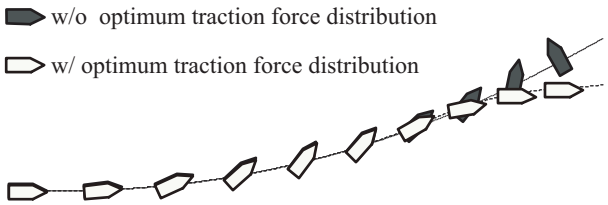

Fig. 15. "Lane change" trajectory of EV controlled by different methods($V = 60km/h$)

dancy of control inputs. That method bring advantages over control strategies which do not use control inputs redundancy.

Futher, using redundancy of control inputs will have more metrits. For example, tire friction constraints can be taken into account, control reconfiguration can be performed when motor failure, and algorithm calculating time can be saved because of the two control loops design.

For future work, this control strategy need to be refined and examined by more experiments. The singularity problem of optimal dynamic redundancy resolution need to be discussed. Because **LQG** regulator is a full state feedback controller, more research should be focused on some observers for the estimation of slip angle β or cornering power, which are difficult to know in real time[14].

REFERENCES

[1] Yoichi Hori, "Future Vehicle driven by Electricity and Control -Research on 4 Wheel Motored 'UOT March II'," *IEEE Transactions on Industrial Electronics*, Vol. 51, No. 5, pp. 954–962, 2004.10.

[2] J. Marshall, M. Kazerani, "Design of an Efficient Fuel Cell Vehicle Drivetrain, Featuring a Novel Boost Converter," *The 31st Annual Conference of the IEEE Industrial Electronics Society*, Raleigh, North Carolina, USA, 2005. 11.

[3] Y. Furukawa and M. Abe, "Direct yaw moment control with estimating side-slip angle using on-board-tire-model," in *Proc. AVEC'98*, Nagoya, Japan, 1998.

[4] Shin-ichiro Sakai, Hideo Sado and Yoichi Hori, "Motion control in an electric vehicle with 4 independently driven in-wheel motors," *IEEE Trans. on Mechatronics*, Vol. 4, No. 1, pp. 9–16, 1999.

[5] Peng He, Yoichi Hori, "Resolving Actuator Redundancy for 4WD Electric Vehicle by Sequential Quadratic Optimum Method," *The 19th Japan Industry Applications Society Conference*, Fukui, Japan, 2005.8.

[6] Peng He, Yoichi Hori, Makoto Kamachi, Kevin Walters and Hiroaki Yoshida, "Future Motion Control to be Realized by In-wheel Motored Electric Vehicle," *The 31st Annual Conference of the IEEE Industrial Electronics Society*, Raleigh, North Carolina, USA, 2005. 11.

[7] Hiroshi Fujimoto, Akio Tsumasaka and Toshihiko Noguchi, "Direct Yaw-moment Control of Electric Vehicle Based on Cornering Stiffness Estimation," *The 31st Annual Conference of the IEEE Industrial Electronics Society*, Raleigh, North Carolina, USA, 2005. 11.

[8] Buffington, J. M., "Tailless aircraft control allocation," *AIAA Guidance, Navigation, and Control Conference and Exhibit*, New Orleans, LA, 1997.

[9] Omerdic, E. and G.N. Roberts, "Thruster fault diagnosis and accommodation for open-frame underwater vehicles," *Special feature GCUV 2003, Control Engineering Practice*, 2004.

[10] Y.Hattori, K.Koibuchi, and T. Yokoyama, "Force and moment control with nonlinear optimum distribution for vehicle dynamics," *In Proc. of the 6th International symposium on advanced vehicle control*, Hiroshima, 2002.

[11] John Harris Plumlee, "Multi-Input Ground Vehicle Control Using Quadratic Programming Based Control Allocation Techniques," *Master thesis*, The Graduate Faculty of Auburn University, Auburn University, 2004.8.

[12] John A. M. Petersen, Marc Bodson, "Constrained Quadratic Programming Techniques for Control Allocation," *Proceedings of the* 42^{nd} *IEEE Conference on Decision and Control*, Maui, Hawaii, USA, 2003.12.

[13] Ola Harkegard, "Backstepping and Control Allocation with Applications to Flight Control," *Ph.D. Thesis*, Submitted to the Department of Electrical Engineering, Linkoping University, Linkoping, Sweden, 2003.

[14] Yoshifumi Aoki, Toshiyuki Uchida, Yoichi Hori, "Experimental Demonstration of Body Slip Angle Control based on a Novel Linear Observer for Electric Vehicle,"*The 31st Annual Conference of the IEEE Industrial Electronics Society*, Raleigh, North Carolina, USA, 2005. 11.